



HAL
open science

Toward oxygen fully stoichiometric $\text{La}_{1-x}\text{Sr}_x\text{CoO}_3$ ($0.5 \leq x \leq 0.9$) perovskites: Itinerant magnetic mechanism more than double exchange one's

Madhu Chennabasappa, Emmanuel Petit, Olivier Toulemonde

► **To cite this version:**

Madhu Chennabasappa, Emmanuel Petit, Olivier Toulemonde. Toward oxygen fully stoichiometric $\text{La}_{1-x}\text{Sr}_x\text{CoO}_3$ ($0.5 \leq x \leq 0.9$) perovskites: Itinerant magnetic mechanism more than double exchange one's. *Ceramics International*, 2020, 46 (5), pp.6067-6072. 10.1016/j.ceramint.2019.11.067 . hal-02613653

HAL Id: hal-02613653

<https://hal.science/hal-02613653>

Submitted on 20 May 2020

HAL is a multi-disciplinary open access archive for the deposit and dissemination of scientific research documents, whether they are published or not. The documents may come from teaching and research institutions in France or abroad, or from public or private research centers.

L'archive ouverte pluridisciplinaire **HAL**, est destinée au dépôt et à la diffusion de documents scientifiques de niveau recherche, publiés ou non, émanant des établissements d'enseignement et de recherche français ou étrangers, des laboratoires publics ou privés.

Toward oxygen fully stoichiometric $\text{La}_{1-x}\text{Sr}_x\text{CoO}_3$ ($0.5 \leq x \leq 0.9$) perovskites: itinerant magnetic mechanism more than double exchange one's

C. Madhu^{a,b}, E. Petit^a, O. Toulemonde^{a*}

^aCNRS, Univ. Bordeaux, Bordeaux INP, ICMCB UMR 5026, Pessac, F-33600, France

^bactual address Department of Physics, Siddaganga Institute of Technology, Tumakuru - 572103, India

*Author Email Address: olivier.toulemonde@icmcb.cnrs.fr

ABSTRACT

We report a two steps synthesis of strontium rich cobaltates $\text{La}_{1-x}\text{Sr}_x\text{CoO}_{3-\delta}$ ($0.5 \leq x \leq 0.9$) compounds. Following the standard solid state procedure, an oxygen intercalation process has been carried out. All the compounds show a perovskite related type structure. Samples have been characterized from chemical and structural point of view. The cubic “a” cell parameter saturates with the oxygen deficiency parameters δ that is controlled by the thermodynamic parameters (p_{O_2} ; T). The magnetic properties studies were carried out before and after oxygen intercalation process and a continuous transfer from a localized character to an itinerant one's when oxygen is up taken is supported. A complete magnetic phase diagram with respect to temperature is proposed. One further evidence for attaining of $\text{Co}^{+3.58}$ against $\text{Co}^{+3.70}$ in $\text{La}_{0.3}\text{Sr}_{0.7}\text{CoO}_{3-\delta}$ with the help of electrochemical oxidation that definitively both metal like behavior and higher than 280K paramagnetic to ferromagnetic temperature phase transition unambiguously signed an oxygen stoichiometry close to 3 in $\text{La}_{1-x}\text{Sr}_x\text{CoO}_3$ perovskites serie.

KEYWORDS $\text{La}_{1-x}\text{Sr}_x\text{CoO}_3$ perovskite ; Cobaltates ; Double exchange ; Itinerant magnetism ; Electrochemical oxidation

Introduction

It is crucial to control the exact oxygen content for a fixed cationic composition ABO_3 (where A = divalent alkaline earth or trivalent rare earth and B = transition metal) exhibiting a perovskite-like structure, to be able to tune the physical properties. Indeed, metal to insulator¹, semiconductor to superconductor² and/or antiferromagnetic to ferromagnetic phases transitions³ can occur from such oxygen content control. Our study is focussed on $La_{1-x}Sr_xCoO_{3-\delta}$ compounds for which the oxygen stoichiometry control is often in relation with the cobalt spin states characterisation due to the large degree of freedom given by Co^{3+} and Co^{4+} from low- to intermediate-and high-spin states. It then opens a way to spin state control for thermochromism properties⁴, electrocatalytic properties^{5,6} and/or switchable device⁷.

Owing to further illustrate the high potential of oxygen intercalation thanks to our electrochemical oxidation set up, we concentrate our investigations on quasi fully stoichiometric $La_{1-x}Sr_xCoO_3$ ($0.5 \leq x \leq 0.9$) oxides showing ferromagnetic metallic properties around room temperature⁸. The communication is organized as follows. In the first section, as-prepared and electrochemical oxidized perovskites chemical analyses and nuclear structures are presented. Then, in the second section, changes in the magnetic properties from the as-prepared to the almost fully oxidized phases are described proposing for the first time a complete magnetic phase diagram in the Sr rich $La_{1-x}Sr_xCoO_3$ ($0.5 \leq x \leq 0.9$) perovskite. Finally, our study shed light on the observed discrepancies when itinerant electrons or ionic spin state models are considered.

Experimental section

Synthesis. Samples $La_{1-x}Sr_xCoO_{3-\delta}$ ($0.5 \leq x \leq 0.9$) were prepared by solid state route using stoichiometric amounts of $SrCO_3$, La_2O_3 and Co_3O_4 ; $SrCO_3$ was stored in an oven at $250^\circ C$ and La_2O_3 was pre heated at $1000^\circ C$ and weighed following a quenching procedure in order to avoid any rehydration. Mixed powders were first annealed for 12 hours in air at $900^\circ C$ for $SrCO_3$ decarbonation and then heated for 14 hours in air at $1150^\circ C$ with intermediate grinding in an agate mortar. The as-stabilized powders were then pressed into pellets for the last heat treatment for 40 hours at $1200^\circ C$. Samples with $0.5 \leq x \leq 0.7$ were fired under oxygen flow during that last heat cycle and cooled down to room temperature at $300^\circ C/hours$ rate and those with $0.8 \leq x \leq 0.9$ are heat treated under argon flow, followed by quenching. Once derived perovskite crystalline phases were obtained and confirmed by X-ray diffraction analysis, the so-called “as prepared” pellets were oxidized in our electrochemical set up. Details of the experiments have already been published^{9,10}. Oxygen was intercalated into oxide networks at room temperature in a galvanostatic mode with a constant current intensity of about $100\mu A$. The oxygen intercalation was followed thanks to chronopotentiometric curves and stopped once the working potential reached a constant value around $500mV$.

Chemical compositions were determined for the as prepared powder oxides by inductively coupled plasma Optical Emission Spectrometer (ICP-OES) on a Varian 720 ES instrument. Powder samples (~ 10 mg) were dissolved in a high-quality hydrochloric acid solution heated at 343 K with constant stirring and the resulting clear solution was analyzed using ICP-OES.

Oxygen Content. The oxidation state distribution of the transition element and then the oxygen

stoichiometry was deduced by iodometric titration¹¹.

Powder X-ray Diffraction. Structural characterization of the samples was made by X-ray diffraction (XRD) employing a Philips PW 1820 apparatus equipped with a $K\alpha_1/K\alpha_2$ source and a copper anticathode. Diffraction patterns were collected with a 2θ step of 0.02° between 8° and 80° with a counting rate of 2s per step in the routine mode. The structures were studied by full pattern matching of the corresponding diagrams. To estimate the cell parameters uncertainties, the mathematic errors given by the Le Bail profile refinement has been multiplied by 3 times the SCOR value extracted from the Pawley's formula.

Physical Properties. DC magnetic susceptibility measurements were performed over the temperature range 2–300 K, using a Squid Quantum Design XL-MPMS magnetometer in zero-field-cooling (ZFC) and field-cooling (FC) conditions. The sample was introduced at room temperature and cooled down in zero-field at 5K/min before the magnetic field was applied. Resistivity measurements were carried out using a home-made four-probe dc setup.

Results

As shown in the table 1, a very slight strontium deficiency is determined by ICP with respect to the targeted stoichiometry. And, a large Co^{4+} oxidation state content is already reached by thermal treatment under O_2 flow as seen from the iodometric titration results. It can be noticed that Co^{4+} contents for $0.5 \leq x \leq 0.7$ compounds are in the same range and that they are even higher than those already reported previously^{12,13,14}. Finally, highest Co^{4+} contents are reached after electrochemical oxidation.

The experimental XRD patterns of the as prepared samples are represented in Figure 1 whereas those obtained after electrochemical oxidation are summarized Figure 2. In both figures, all the main peak diffraction patterns are about at the same 2θ values indicating quite uniform interplanar spacings for each XRD series. Profile analysis was performed on all the samples. The phase distributions are summarized in table 1. Based on composition and sample, three phases can be identified: the main cubic perovskite crystallizing in $Pm\bar{3}m$ space group, the competing phase $(\text{La,Sr})_2\text{CoO}_4$, note that profile fitted x-ray diffraction patterns for both $\text{La}_{0.4}\text{Sr}_{0.6}\text{CoO}_{3-\delta}$ compounds are shown in supplementary figure S1 due to its higher content of $(\text{La,Sr})_2\text{CoO}_4$ phase, and finally the strontium carbonate that is formed during electrochemical oxidation and mainly for high concentration of Sr ($0.8 \leq x \leq 0.9$). Let us recall that electrochemical oxidations were carried out on the same powder batches than the as prepared ones which will then be first emphasized.

Targeted Sr Content	Phase distribution		Analysis ICP-OES results (normalized to Co content)		Iodometric titration results			Sample synthesis
	Phase I (%)	Phase II (%)	La/Co	Sr/Co	δ	Co ⁴⁺ content		
						Expected if $\delta=0$	Estimated for titrated δ	
0.5	100 98.5	0.00 1.5 ⁺	0.50	0.48	0.07 0.03	50%	37% 44%	As prepared Electrochemistry oxidized
0.6	100 95.7	0.0 2.9 ⁺ , 1.5 ^{\$}	0.39	0.62	0.07 0.03	60%	46% 54%	As prepared Electrochemistry oxidized
0.7	99.5 99.3	0.5 ⁺ 0.8 ⁺	0.30	0.69	0.14 0.06	70%	42% 58%	As prepared Electrochemistry oxidized
0.8	-- 95.4	-- 0.8 ⁺ , 3.8 ^{\$}	0.20	0.78	0.37 0.08	80%	6% 64%	As prepared Electrochemistry oxidized
0.9	-- 83.3	-- 1.2 ⁺ , 15.5 ^{\$}	0.10	0.88	0.47 0.17	90%	0% 56%	As prepared Electrochemistry oxidized

1st phase is the main cubic perovskite structure referring to the magnetic phase.
2nd phase ⁺ is the (La,Sr)₂CoO₄ based tetragonal phase
3rd phase ^{\$} is SrCO₃.

Table 1 : XRD Profile and ICP-OES analyses and Iodometric titration results for La_{1-x}Sr_xCoO_{3- δ} (0.5 ≤ x ≤ 0.9) oxides following the different step of the electrochemical oxidation process.

Oxygen flow annealed oxides for 0.5 ≤ x ≤ 0.7 show cubic perovskite type structure with sometimes a tiny peak indicating a (La_ySr_x)₂CoO₄ secondary phase. Cell parameters values obtained after the Le Bail refinements are collected together in Table 2. It can be pointed out that for 0.5 ≤ x ≤ 0.7 compounds, the refined “a” cell parameter is equivalent than those reported^{6,14}. The cubic cell parameters are almost constant whatever the Sr/La ratio is. This result has to be seen regarding the almost constant Co⁴⁺ content reached: our XRD patterns do not followed the expected change when the ionic radii model is considered. Contrary, those annealed under argon flow and quenched show mixed brownmillerite and cubic perovskite structure for 0.8 ≤ x ≤ 0.9. The brownmillerite refinements were carried out using Imma model¹⁵.

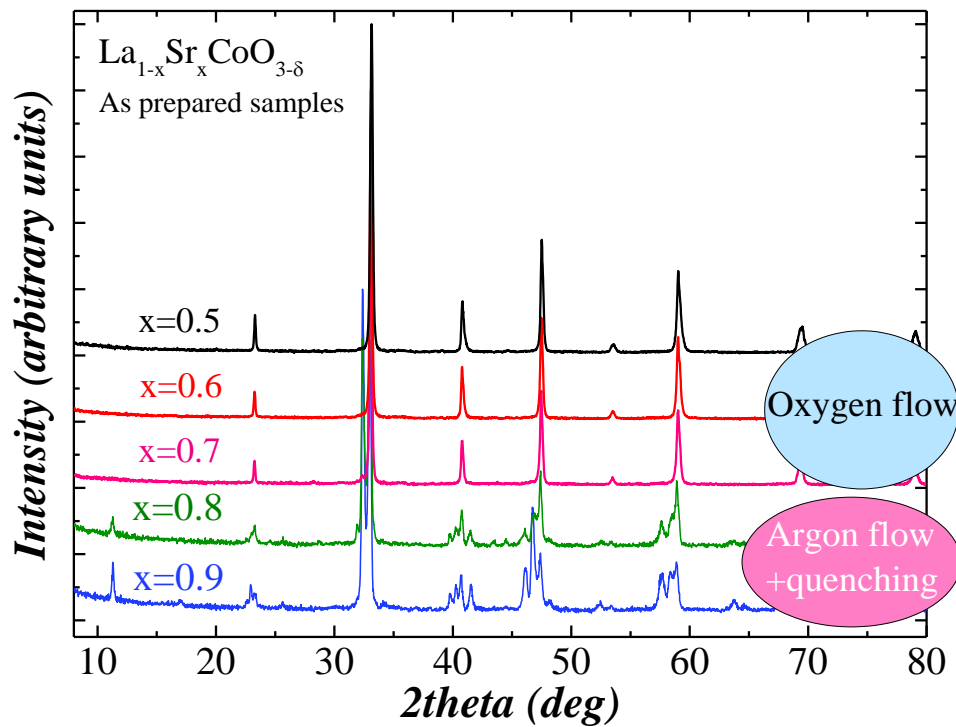


Figure 1 : X-ray diffraction (XRD) patterns for the as prepared $\text{La}_{1-x}\text{Sr}_x\text{CoO}_3$ ($0.5 \leq x \leq 0.9$) obtained following the described experimental procedure.

Targeted Chemical composition	Cell parameters (Å)	Oxygen deficiency δ	Curie Temperature (1 st derivative) ($\pm 5\text{K}$)	Average spin value	Paramagnetic Temperature
$\text{La}_{0.5}\text{Sr}_{0.5}$	3.8322 (16)	0.07	250K	1.74	255K
$\text{La}_{0.4}\text{Sr}_{0.6}$	3.8326 (08)	0.07	250K	1.76	275K
$\text{La}_{0.3}\text{Sr}_{0.7}$	3.8320 (07)	0.14	265K	1.60	270K

Table 2: Principals physicochemical properties for the as prepared sample

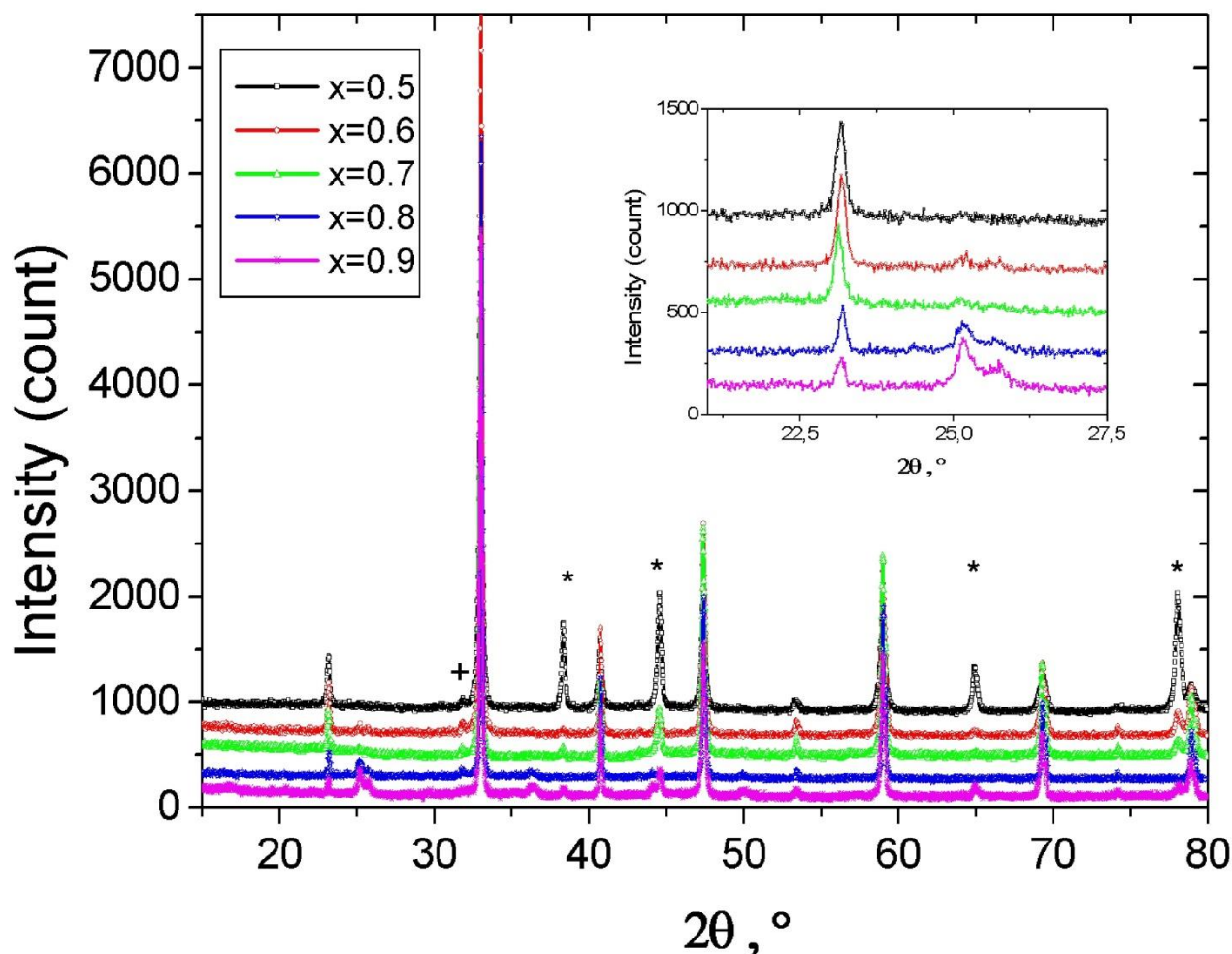


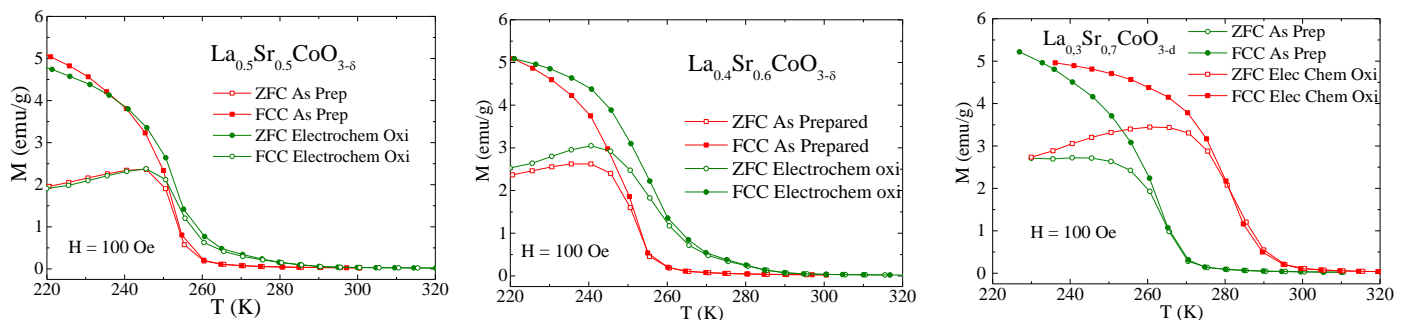
Figure 2 : X-ray diffraction (XRD) patterns for the electrochemically oxidized $\text{La}_{1-x}\text{Sr}_x\text{CoO}_3$ ($0.5 \leq x \leq 0.9$); the tiny peak denoted by + likely indicates a $(\text{La}_y\text{Sr}_x)_2\text{CoO}_4$ secondary phase⁶ ; the peaks denoted by * indicate the Al sample holder support that can be used as standard. The perovskite type structure (100) Bragg peak and the main SrCO_3 phase peak around $2\theta=25^\circ$ are shown in the insert.

Targeted Chemical composition	Cell parameters (Å)	Oxygen deficiency δ	Curie Temperature (1 st derivative)	Average spin value	Paramagnetic Temperature
$\text{La}_{0.5}\text{Sr}_{0.5}$	3.8250 (28)	0.03	255K	1.91	260K
$\text{La}_{0.4}\text{Sr}_{0.6}$	3.8279 (14)	0.03	255K	1.67	257K
$\text{La}_{0.3}\text{Sr}_{0.7}$	3.8245 (15)	0.06	280K	1.51	295K
$\text{La}_{0.2}\text{Sr}_{0.8}$	3.8288 (08)	0.08	275K	1.47	285K
$\text{La}_{0.1}\text{Sr}_{0.9}$	3.8297 (21)	0.17	275K	1.51	292K

Table 3: Principals physicochemical properties after chemical oxidation process.

With oxygen intercalation, as illustrated in figure 2, all the patterns can be now indexed within a cubic perovskite form ($Pm\bar{3}m$ space group). An increase of the SrCO_3 secondary phase with the strontium content is noticed. Quite uniform cell parameters are still observed as illustrated both in the inset of figure 2 and in Table 3. However, as expected a smaller “a” cell parameters are reported when oxygen deficiency decreases. In average, it goes from $\langle a \rangle = 3.8323 \text{ \AA}$ for the as prepared oxides to $\langle a \rangle = 3.8272 \text{ \AA}$ for the electrochemical oxidized ones. The titrated oxygen deficiency and the cell parameter increase from $x = 0.7$ to $x = 0.9$, both suggest that O^{2-} intercalation is not fully completed. It is likely mainly due to CO_2 adsorption during the electrochemical oxidation as observed in the diffractograms. However, especially for $\text{La}_{0.2}\text{Sr}_{0.8}\text{CoO}_3$ oxide, our “a” cell parameter is slightly lower than this reported¹⁶ supporting a successful electrochemical oxidation process.

As illustrated in figure 3 for $0.5 \leq x \leq 0.7$, all the cubic cobaltite perovskites show paramagnetic to ferromagnetic phase transition. Phase transition temperatures depend on either the La/Sr ratio or the oxygen content as summed up in table 2 & 3. When a high Co^{4+} content was already stabilized for $x=0.5$ and/or 0.6, not much significant changes in the magnetic properties are observed between as prepared and oxidized compounds, the electrochemical oxidation not seems to be highly relevant. Only a slight loss of the abruptness of the phase transition which becomes broader is seen. By contrast for $x=0.7$, the phase transition temperature is significantly higher when electrochemical oxidation is carried out and the abruptness of the phase transition is kept. For as prepared $x=0.8$ & $x=0.9$ oxides, magnetic characterisation were not performed due to phase separation. A high antiferromagnetic ordering temperature is reported for brownmillerite ($T_N = 537 \text{ K}$ for $\text{Sr}_2\text{Co}_2\text{O}_5$ ¹⁷) that is expected to be mixed with a lower ordering temperature for the cubic oxygen disordered phase. When they are oxidized by electrochemistry process, the two oxides behave as the formers with a paramagnetic to ferromagnetic phase transition occurring at temperatures as high as the other oxides. Interestingly, our estimated phase transition temperature are higher than those already reported in literature^{12,16} further supporting the success of our electrochemical oxidation process. Phase transition temperature of our samples are about the same than that reported for SrCoO_3 ¹⁸ with $T_C = 280 \text{ K}$. Unfortunately, such high unusual oxidation state is not stable in time as highlighted in the data collected 8 months later the first collection for $\text{La}_{0.2}\text{Co}_{0.8}\text{CoO}_{3-\delta}$ compounds. Such redox phenomenon has already been reported for $\text{SrFe}_{0.5}\text{Co}_{0.5}\text{O}_{3-\delta}$ compounds¹⁰.



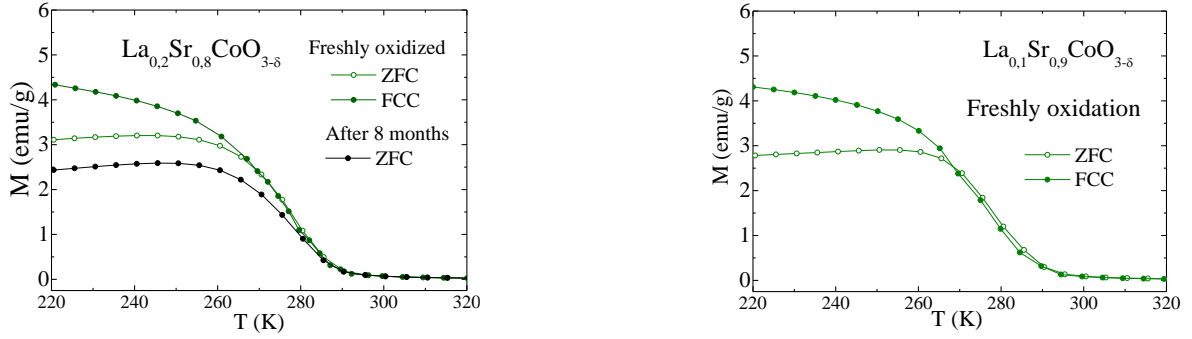


Fig 3: Magnetization curves for $\text{La}_{1-x}\text{Sr}_x\text{CoO}_3$ ($0.5 \leq x \leq 0.9$) samples as function of temperature in both ZFC and FCC mode under constant magnetic field 100 Oe.

Finally, in the paramagnetic range, all the magnetic susceptibility were fitted thanks to a Curie Weiss law allowing an average spin value estimation from the slope and a Paramagnetic temperature one's from the intercept (see table 2 & 3). The extracted average spin values continuously decreases when Co^{4+} content increase. And, they are always higher than the expected ones assuming an ionic model with Co^{4+} in an intermediate spin state $S = \frac{1}{2}$ ^{8,19} with a rate equal to the Sr content and some Co^{3+} in a high spin state $S=2$ with a rate equal to the La^{3+} content. Having in mind the ferromagnetic/metallic properties observed for $0.2 < x < 0.7$, in contrast with the proposed thermally driven spin state transition⁸, our results better support a continuous change of the localized electrons content up to saturation in relation with the number of introduced Co^{4+} during the electrochemical oxidation.

Discussion

Paraelastic/cubic to ferroelastic/rhomboedric phase transition has already been pointed out when $x \leq 0.5$ ²⁰. In parallel, a continuous increase in cobalt oxidation state occurs from Co^{3+} to $\text{Co}^{3.5+}$ when prepared under dioxygen flow. When Sr content is further increased, our study does not report any significant changes in the Co oxidation state as already supported by literature¹³. The cationic charges difference from La^{3+} to Sr^{2+} is better compensated by oxygen vacancies formation than cobalt oxidation. Thus the observed cubic phases by XRD are definitively significant of oxygen vacancies disordering. In the ordered vacancies related structure called brownmillerite, isolated MO_4 tetrahedral are in zigzag chains alternatively with octahedral layers. Within the tetrahedral layers, the chain rotations may be ordered (*Pnma* or *I2mb* symmetry) or disordered (*Imma* symmetry) with respect to adjacent layers as previously well described¹⁵. Not shown XRD profiles matching were refined using a disordered chain rotation model mixed with a disordered oxygen vacancies one's. Unfortunately, our XRD data collection do not allow us to propose if any chain rotation ordering phase transition with respect to the $\text{Sr}^{2+}/\text{La}^{3+}$ ratio in the A-site perovskite occurs. However, the as obtained cubic and brownmillerite mixed phases may suggest that lanthanum introduction would act as oxygen disordering vacancies driving force. Out of the topic of our study, no specific experiments were carried out to stabilize single brownmillerite type structure when La^{3+} is introduced.

LaCoO_3 is known to show a low spin to higher spin state cross over²¹ supporting localized electrons contrary to SrCoO_3 showing ferromagnetic properties resulting from the itinerant σ^*e_g electrons with the quasilocated t_{2g} ones coupling¹⁸. When $\text{La}_{1-x}\text{Sr}_x\text{CoO}_3$ is carried out, an insulator to metal-like transition occurs when x reach about 0.2 in relation with the progressive crystalline phase transition from rhombohedral to cubic form¹². Air and/or oxygen annealing procedure allow stabilizing

stoichiometric phase which show metallic properties for $0.2 \leq x \leq 0.5$ ²². However, the metallic properties are gradually lost with oxygen vacancies introduction^{12,14} and the ferromagnetic to paramagnetic temperature phase transition was reported at a maximum for $x = 0.5$ attaining 250K as shown figure 4.

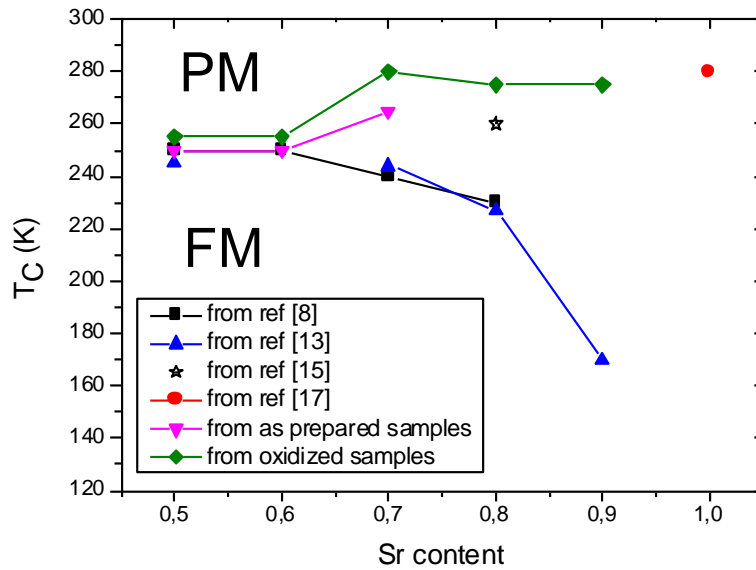


Figure 4 : Magnetic phase diagram in a Temperature - Sr content plan for $\text{La}_{1-x}\text{Sr}_x\text{CoO}_3$ ($0.5 \leq x \leq 1$).

**PM = Paramagnetic phase,
FM = Ferromagnetic phase**

lines are guided for eyes

Our results unambiguously converge towards previous studies up to $x = 0.6$ but one succeed to reach T_C as high as 265K for as prepared $x=0.7$ oxide under O_2 flow. J. Wu and C. Leighton⁸ were suggesting that a maximum of $T_C = 250\text{K}$ for $x=0.5$ was related to the 1:1 ratio for Co^{3+} to Co^{4+} maximizing the strength of the double exchange interactions. However, our results do not support a continuous change of the “a” cell parameter in relation with the Goldschmidt factor but a quasi-constant “a” cell parameter is reported whatever the $\text{Sr}^{2+}/\text{La}^{3+}$ ratio is. Such quasi-constant cell parameter phenomenon has already been reported for ferromagnetic-metallic $\text{SrFe}_{1-x}\text{Co}_x\text{O}_3$ oxides²³ when itinerant electrons are involved in. Furthermore, even if the maximum oxygen stoichiometry might not be attained because of CO_2 adsorption during the electrochemical process, one even highlights T_C as high as 280K for electrochemically oxidized $\text{La}_{0.3}\text{Sr}_{0.7}\text{CoO}_3$ oxide as observed in SrCoO_3 ¹⁸. The maximum Curie temperature would thus not be related to double exchange involving electron hopping through double-exchange mechanism to correlate the ferromagnetic properties with the metallic one’s. If one considers the model involving anion to cation charge transfer^{6,12,14}. Electronic conductivity of $\text{La}_{1-x}\text{Sr}_x\text{CoO}_3$ is improved with Sr^{2+} because the cobalt oxidation state increases resulting in hole introduction up to a maximum that may be in relation with oxygen vacancies formation when $x > 0.5$. And, an enhancement of the overlap occurs between the occupied O 2p valence bands and the unoccupied Co 3d conduction bands leading to possible anion to cation charge transfer¹⁴. Such overlapping in relation with anion to cation charge transfer phenomenon is well characterized by O K-edge X-ray absorption spectroscopy²⁴. However, it has already been pointed out that such picture cannot change the magnetic properties. Indeed such anion to cation charge transfer results in a spin density transfer from cation to anion as already probed by X-ray magnetic circular dichroism at OK-edge²⁵ but cannot explained a magnetic moment as high as $2.1\mu_B$ measured in SrCoO_3 ¹⁸. That is why our magnetic properties are better explained by the itinerant model proposed by Bezducka and co-worker¹⁸ which was later picked up for

Sr poor $\text{La}_{1-x}\text{Sr}_x\text{CoO}_3$ ($0.5 \leq x \leq 0.5$) perovskites perovskite²⁶. In order to explain such high magnetic moment of $2.1\mu_B$, a partial charge transfer from t_{2g}^{down} to e_g^{up} has to be considered. If x estimates the fraction of electrons in the e_g^{up} orbitals, it has to be equal to $\frac{1}{2}$ to reach a magnetic saturation equal to $2\mu_B$. It indeed agrees Medling and co-workers conclusions²⁵ suggesting a mixture of filled e_g and t_{2g} states. It is from the delocalization of such d electrons in the $\sigma^*e_g^{\text{up}}$ band than the metallic character is understood and from the quasi localized electron in the t_{2g}^{down} ferromagnetically coupled with the itinerant σ^*e_g electrons that the magnetic properties are explained. It would give an electron distribution for each cobalt $t_{2g}^{5-x}e_g^x$ with x being the fraction of electrons in the e_g orbitals. In the case of $\text{Sr}_{0.7}\text{La}_{0.3}\text{CoO}_3$, it turns out from our iodometric titration that the Co^{4+} content increases from 42% to 58% giving an average cobalt oxidation state increase from $\text{Co}^{+3.42}$ to $\text{Co}^{+3.58}$ for a maximum expected equal of $\text{Co}^{+3.70}$. Thereby, $\text{Sr}_{0.7}\text{La}_{0.3}\text{CoO}_3$ material shifts from semi-conducting behavior to metal-like when oxidized but with a room temperature resistance value in the same range as oxygen deficient. It only decreases by a factor 3 (fig. 5a). As seen in figure 5b, the magnetic moment slightly increases with the oxidation process under 4T at 5 K from 46.90 emu/gr ($1.73\mu_B/\text{Co}$) to 50.14 emu/gr ($1.85\mu_B/\text{Co}$). Assuming the itinerant model proposed by Bezduka and co-worker¹⁸ giving $M^{\text{sat}}=(1+2x)$, even if magnetization saturation is not fully complete, it corresponds to an increase of delocalized electrons fraction from 0.365 to 0.425 which well agree the localized electrons decrease estimated from the slope of the Curie Weiss law when $\langle S \rangle$ goes from 1.6 to 1.5.

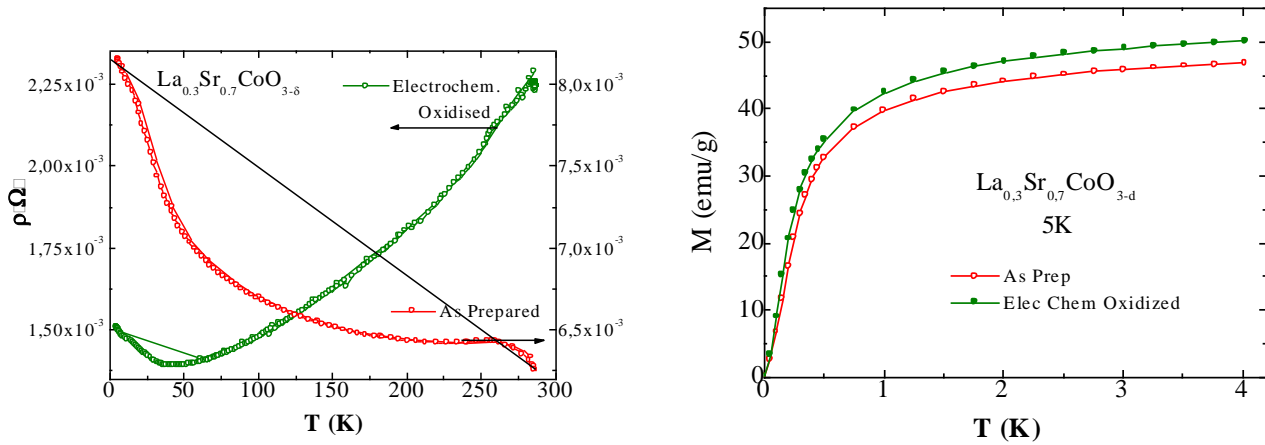


Figure 5 : (a) Resistance temperature dependance that were collected in the same pellet before and after the electrochemical oxidation process and (b) magnetization isothermal for $\text{La}_{0.3}\text{Sr}_{0.7}\text{CoO}_3$ in as prepared and after oxidation process.

Finally, if one refers to the V. Pralong and co-worker study¹⁶, they reported a magnetic moment equal to $1.95 \mu_B/\text{Co}$ at 5 K with applied field of 5 T, a paramagnetic to ferromagnetic transition temperature of about 260K (extracted from the inflection point to compare with our data), a cell parameter $a = 3.8355\text{\AA}$ and a room temperature resistivity $\rho_{300\text{ K}} = 1.6 \text{ m}\Omega \text{ cm}$. All these results perfectly match with our study suggesting a delocalized electrons fraction of about 0.475 in between $\text{Sr}_{0.7}\text{La}_{0.3}\text{CoO}_3$ and SrCoO_3 . In conclusion of our discussion, both a metal like behavior and a paramagnetic to ferromagnetic temperature phase transition around 280K are unambiguous results from an oxygen stoichiometry close to 3 in rich strontium $\text{La}_{1-x}\text{Sr}_x\text{CoO}_3$ perovskites.

Conclusion

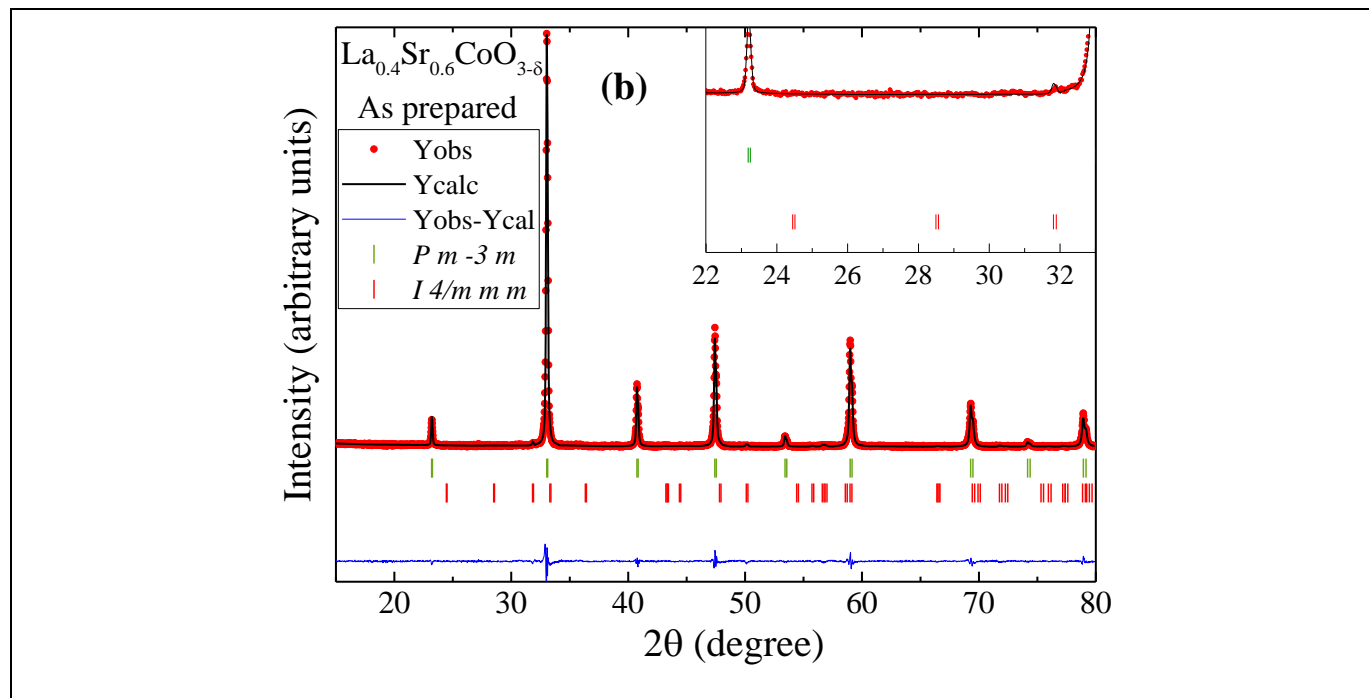
Almost fully stoichiometric of rich strontium $\text{La}_{1-x}\text{Sr}_x\text{CoO}_{3-\delta}$ ($0.5 \leq x \leq 0.9$) compounds were prepared demonstrating once again the high efficiency of the electrochemical process. Chemical analyses and physical properties of the different compounds showing ferromagnetic behavior up to 280 K and metallic conductivity confirm it. Magnetization studies better support an itinerant magnetic mechanism involving a partial charge transfer from t_{2g}^{down} to e_g^{up} than an occupied O 2p valence bands to the unoccupied Co 3d conduction bands charge transfer or double exchange phenomena. Our study would even suggest that higher than 280K paramagnetic to ferromagnetic phase transition temperature might be obtained if one succeeds to limit CO_2 adsorption during electrochemical oxidation process. The ferromagnetic to paramagnetic temperature phase transition around room temperature would suggest the possible used of these oxides for magnetic refrigeration

ACKNOWLEDGMENT R. Decourt, E. Lebraud and L. Etienne for their technical assistance in resistance, ICP- OES and XRD data collection & E. Gaudin and M. Pollet for fruitful scientific discussion respectively.

This work has been supported by the European project “SOPRANO” under Marie Curie actions (Grant No. PITNGA-2008-214040).

MC likes to acknowledge Université de Bordeaux for his Ph.D. fellowship.

Supplementary Information



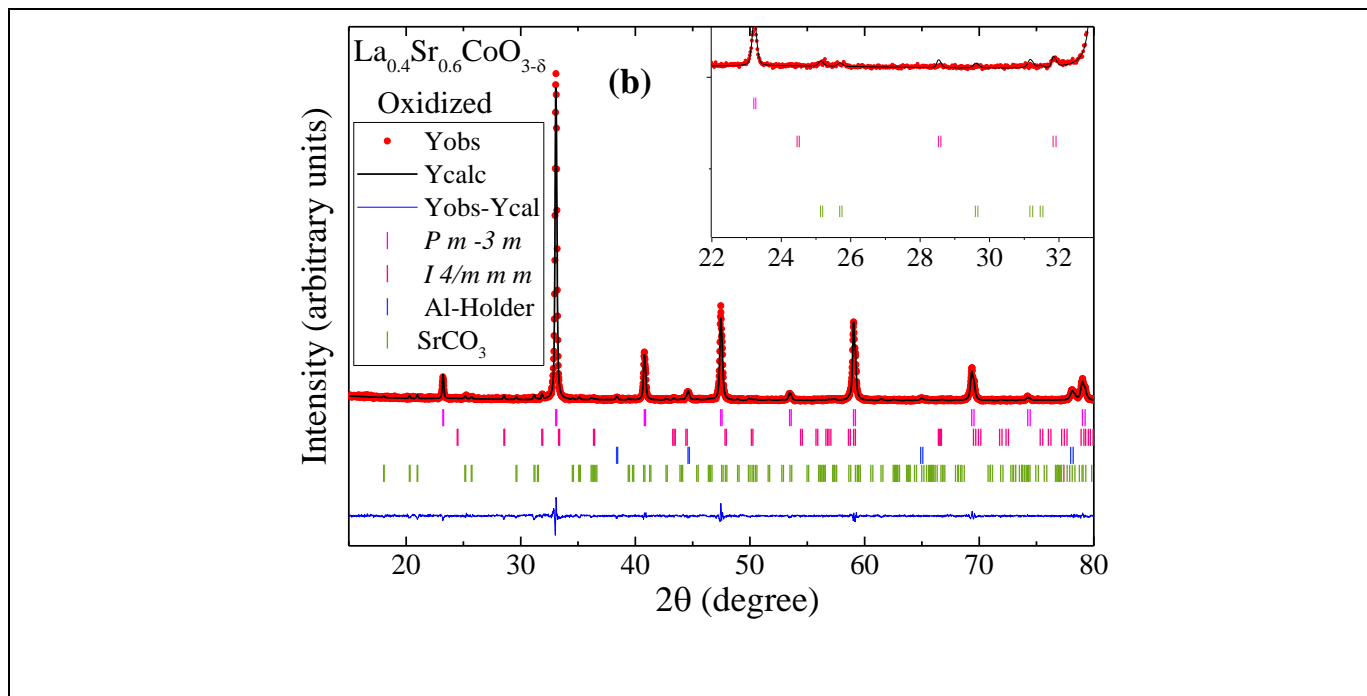


Figure S 1: Profile fitted x-ray pattern for (a) as prepared and (b) Electrochemical oxidized $\text{La}_{0.4}\text{Sr}_{0.6}\text{CoO}_{4-\delta}$

- ¹ A. Lebon, P. Adler, C. Bernhard, A. V. Boris, A. V. Pimenov, A. Maljuk, C. T. Lin, C. Ulrich, and B. Keimer, Magnetism, charge order, and giant magnetoresistance in $\text{SrFeO}_{3-\delta}$ single crystals Phys. Rev. Lett. 92 (2004) 037202
- ² D. Barbut, A. Wattiaux, M.H. Delville, J.C. Grenier and J. Etourneau Electrochemical oxidation of La_2CuO_4 in organic media: influence of the electrolyte composition J. Mater. Chem., 12 (2002) 2961
- ³ J. Töpfer and J. B. Goodenough $\text{LaMnO}_{3+\delta}$ Revisited J. Solid State Chem. 130 (1997) 117-128
- ⁴ O.Toulemonde, A. Devoti, P. Rosa, P. Guionneau, M. Duttine, A. Wattiaux, E. Lebraud, N. Penin, R. Decourt, A. Fargues, S. Buffière, A. Demourgues and M. Gaudon Probing Co- and Fe-doped LaMO_3 (M = Ga, Al) perovskites as thermal sensors Dalton Trans. 47 (2018) 382-393
- ⁵ Y.Tong, Y. Guo, P. Chen, H. Liu, M. Zhang, L. Zhang, W. Yan, W. Chu, C. Wu, and Y. Xie Spin-State Regulation of Perovskite Cobaltite to Realize Enhanced Oxygen Evolution Activity Chem. 3 (2017) 812–821
- ⁶ X. Cheng, E. Fabbri, M. Nachttegaal, I. E. Castelli, M. El Kazzi, R. Haumont, N Marzari, and T. J. Schmidt Oxygen Evolution Reaction on $\text{La}_{1-x}\text{Sr}_x\text{CoO}_3$ Perovskites: A Combined Experimental and Theoretical Study of Their Structural, Electronic, and Electrochemical Properties Chem. Mater. 27 (2015) 7662–7672
- ⁷ T. Katase, Y. Suzuki, H. Ohta Reversibly switchable electromagnetic device with leakage-free electrolyte Adv. Electron. Mater. 2 (2016) 1600044
- ⁸ J. Wu and C. Leighton Glassy ferromagnetism and magnetic phase separation in $\text{La}_{1-x}\text{Sr}_x\text{CoO}_3$ Phys. Rev. B 67 (2003) 174408
- ⁹ L.Fournes, A.Wattiaux, A.Demourgues, P. Bezdicka, J.C. Grenier, M. Pouchard and J. Etourneau Investigation of the $\text{SrFe}_{1-x}\text{Co}_x\text{O}_3$ ($0 \leq x \leq 1$) Cubic Perovskites Obtained by Electrochemical Oxidation J. Phys. IV France 07 (1997) C1-353
- ¹⁰ O. Toulemonde, J. Abel, C. Yin, A. Wattiaux, and E. Gaudin Chem. Mater., 24 (2012) 1128–1135
- ¹¹ M. Karppinen, M. Matvejeff, K. Salomaki and H. Yamauchi Oxygen content analysis of functional perovskite-derived cobalt oxides J. Mater. Chem., 12 (2002) 1761–1764
- ¹² A. Mineshige, M. Inaba, T. Yao, and Z. Ogumi Crystal Structure and Metal–Insulator Transition of $\text{La}_{1-x}\text{Sr}_x\text{CoO}_3$ J. Solid State Chem., 121 (1996) 423–429
- ¹³ J. E. Sunstrom IV, K. V. Ramanujachary, and M. Greenblatt, The Synthesis and Properties of the Chemically Oxidized Perovskite, $\text{La}_{1-x}\text{Sr}_x\text{CoO}_{3-\delta}$ ($0.5 < x < 0.9$) J. Solid State Chem., 139 (1998) 388-397
- ¹⁴ J. T. Mefford, X. Rong, A. M. Abakumov, W. G. Hardin, S. Dai, A. M. Kolpak, K. P. Johnston & K. J. Stevenson Water electrolysis on $\text{La}_{1-x}\text{Sr}_x\text{CoO}_{3-\delta}$ perovskite Electrocatalysts Nature Communications 7, (2016) 11053
- ¹⁵ E. Sullivan, J. Hadermann, C. Greaves Crystallographic and magnetic characterisation of the brownmillerite $\text{Sr}_2\text{Co}_2\text{O}_5$ J. Solid State Chem., 184 (2011) 649–654
- ¹⁶ V. Pralong ; V. Caignaert ; S. Hebert ; C. Marinescu ; B. Raveau ; A. Maignan, Electrochemical oxidation and reduction of the $\text{La}_{0.2}\text{Sr}_{0.8}\text{CoO}_{3-\delta}$ phases : Control of itinerant ferromagnetism and magnetoresistance. Solid State Ionics 177 (2006) 815–820

-
- ¹⁷ A. Muñoz, C. de la Calle, J. A. Alonso, P. M. Botta, V. Pardo, D. Baldomir, and J. Rivas Crystallographic and magnetic structure of SrCoO_{2.5} brownmillerite: Neutron study coupled with band-structure calculations Phys. Rev. B 78, (2008) 054404
- ¹⁸ P. Bezdzicka, A. Wattiaux, J. C Grenier, M. Pouchard, and P. Hagenmuller, Preparation and Characterization of Fully Stoichiometric SrCoO₃, by Electrochemical Oxidation, Z. anorg. allg. Chem. 619 (1993) 7-12
- ¹⁹ F. Guillou, Q. Zhang, Z. Hu, C. Y. Kuo, Y. Y. Chin, H. J. Lin, C. T. Chen, A. Tanaka, L. H. Tjeng, and V. Hardy Coupled valence and spin state transition in (Pr_{0.7}Sm_{0.3})_{0.7}Ca_{0.3}CoO₃ Phys. Rev. B 87 (2013) 115114
- ²⁰ J. Mastin, M.A. Einarsrud, and T. Grande, Structural and Thermal Properties of La_{1-x}Sr_xCoO_{3-δ} Chem. Mater. 18 (2006) 6047-6053
- ²¹ C. S. Naiman, R. Gilmore, B. DiBatolo, A. Linz, and R. Santoro, Interpretation of the Magnetic Properties of LaCoO₃ J. Appl. Phys. 36 (1965) 1044
- ²² O.Toulemonde·N.N'Guyen·F.Studer·A.Traverse Spin State Transition in LaCoO₃ with Temperature or Strontium Doping as Seen by XAS J. Solid State Chem., 158 (2001) 208-217
- ²³ S. Kawasaki, M.Takano, Y. Takeda Ferromagnetic Properties of SrFe_{1-x}Co_xO₃Synthesized under High Pressure J. Solid State Chem., 121 (1996)174–180
- ²⁴ F. M. F. de Groot, M. Grioni, J. C. Fuggle, J. Ghijsen, G. A. Sawatzky, and H. Petersen Oxygen 1s x-ray-absorption edges of transition-metal oxides Phys. Rev. B 40 (1989) 5715
- ²⁵ S. Medling, Y. Lee, H. Zheng, J. F. Mitchell, J. W. Freeland, B. N. Harmon, and F. Bridges Evolution of Magnetic Oxygen States in Sr-Doped LaCoO₃ Phys. Rev. Lett. 109 (2012) 157204
- ²⁶ M.A. Señarís-Rodríguez and J.B. Goodenough Magnetic and Transport properties of the system La_{1-x}Sr_xCoO_{3-δ} (0<x≤0.5) J. Solid State Chem., 118 (1995), 323